an ASME publication

$3.00 PER COPY
$1.50 TO ASME MEMBERS

Fracture Mechanics Analysis of JAERI Model Pressure Vessel Test

S. A. DELVIN

Program Engineer

P. C. RICARDELLA

Principal Engineer

General Electric Co.
San Jose, Calif.

A fracture mechanics evaluation of the Japan Atomic Energy Research Institute (JAERI) model pressure vessel experiment was performed using an analytical method which has been used previously to evaluate Boiling Water Reactor feedwater nozzles. Excellent agreement between analysis and experiment was obtained, from which it is concluded that: (a) the test confirms GE predictions of leak-before-break as the hypothetical failure mode, and (b) the fracture mechanics methodology used by GE to predict nozzle crack growth is accurate for the entire range of crack growth, from nucleation to through-wall leakage. These conclusions are particularly significant with regard to very large cracks (greater than 20 percent of nozzle wall thickness) which have never occurred in an operating reactor, but for which the applicability of the method cannot be demonstrated theoretically.

Contributed by the Pressure Vessels & Piping Division of The American Society of Mechanical Engineers for presentation at the Joint ASME/CSME Pressure Vessels & Piping Conference, Montreal, Canada, June 25-30, 1978. Manuscript received at ASME Headquarters April 5, 1978.

Copies will be available until March 1, 1979.

THE AMERICAN SOCIETY OF MECHANICAL ENGINEERS UNITED ENGINEERING CENTER, 345 EAST 47th STREET, NEW YORK, N.Y. 10017

Fracture Mechanics Analysis of JAERI Model Pressure Vessel Test

S. A. DELVIN P. C. RICARDELLA

ABSTRACT

A fracture mechanics evaluation of the Japan Atomic Energy Research Institute (JAERI) model pressure vessel experiment was performed using an analytical method which has been used previously to evaluate Boiling Water Reactor feedwater nozzles. Excellent agreement between analysis and experiment was obtained, from which it is concluded that:

1 The test confirms GE predictions of leak-before-break as the hypothetical failure mode.

2 The fracture mechanics methodology used by GE to predict nozzle crack growth is accurate for the entire range of crack growth, from nucleation to through-wall leakage.

These conclusions are particularly significant with regard to very large cracks (greater than 20 percent of nozzle wall thickness) which have never occurred in an operating reactor, but for which the applicability of the method can not be demonstrated theoretically.

SUMMARY OF JAERI PRESSURE VESSEL TEST

As an integrity assessment for a reactor pressure vessel, the Japan Atomic Energy Research Institute (JAERI) conducted a model pressure vessel experiment to study stress concentration and crack propagation behavior in the vicinity of vessel nozzles (Reference 1). A cyclic internal pressure test was conducted on an approximately one-sixth scale Boiling Water Reactor (BWR) pressure vessel model designed to the criteria of Reference 2. Three types of welded-in nozzles were used in the model. The vessel shell was constructed of low alloy steel, ASTM Type A302 Grade C with nozzles made of a forging steel, ASTM Type A336 Modified. The nozzle blend radius of each nozzle was machined to simulate a flaw which would produce cracking under cyclic pressure load. The internal pressure was cycled from 0 to 10.8 MPa (1566 psi) with oil as the pressurizing agent with a cycling rate of 5 cpm. After 29,200 cycles the test was terminated since one of the artificial cracks (crack type A, nozzle N1) had propagated to the outer surface resulting in oil leakage.

Cross sections of the three nozzle types used are shown in Figure 1. Two of the three nozzle types (N1 and N3) had configurations similar to BWR feedwater nozzles. Two types of artificial cracks were machined into the nozzle blend radius. Type A had a 20-mm (0.787-in.) surface length and a 3-mm (0.118-in.) depth with a straight crack front. Type B had a 8-mm (0.315-in.) surface length and a 3-mm (0.118-in.) depth with a circular arc crack front.

Prior to machining the simulated flaws in the nozzles, a static internal pressure test was conducted in increments to the maximum internal pressure of 10.8 MPa (1566 psi). The stress distributions of the inner and outer nozzle surfaces were determined from strain gages. Elastic stress concentrations were determined assuming Young's Modulus and Poisson's ratio values of 2.06×10^5 MPa (29.87×10^6 psi) and 0.3, respectively. Circumferential stresses and stress concentration factors for the nozzle blend radius are summarized in Table 1.

Table 1. Stress Concentration of Inner Corner Surface of Nozzles

	Nozzle Type N1	N2	N3
Circumferential Stress of Inner Surface of Shell (ksi)	29.3	29.3	29.3
Circumferential Stress of Nozzle Inner Corner Surface (ksi)	71.8	66.1	74.9
Stress Concentration Factor of Nozzle Inner Corner Surface	2.5	2.3	2.6

(ksi) = (6.895 MPa)

The experimental crack growth results obtained in the cyclic testing are summarized in Fig. 2. Fig. 2(a) shows the relationship between crack length measured from the tip of the A-type notch in the N1 nozzle and the number of pressure cycles. Upon examination it can be concluded that the crack propagation rates in the a- and b-directions are greater than that in the c-direction except in the early stages. Fig. 2(b) compares a-direction crack propagation for the three nozzle types. Fig. 2(c) indicates final experimental crack lengths and depths for each notch and nozzle type.

Immediate conclusions which can be drawn from the experiment are as follow:

1 The mode of failure was leak-before-break.

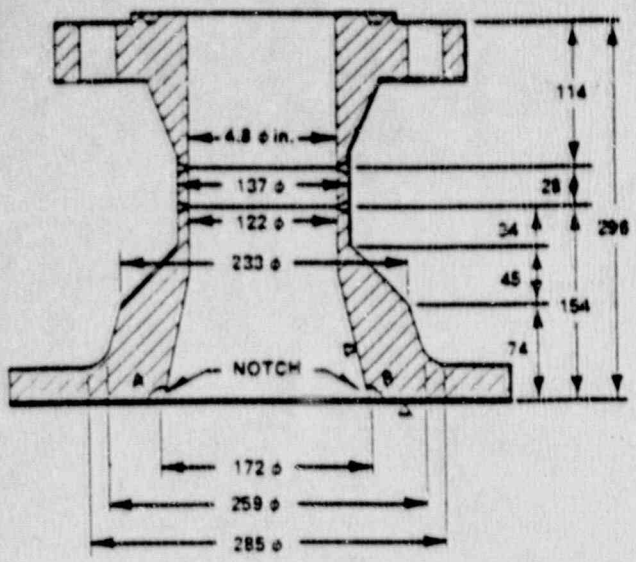

(a) CROSS SECTION OF NOZZLE TYPE N1

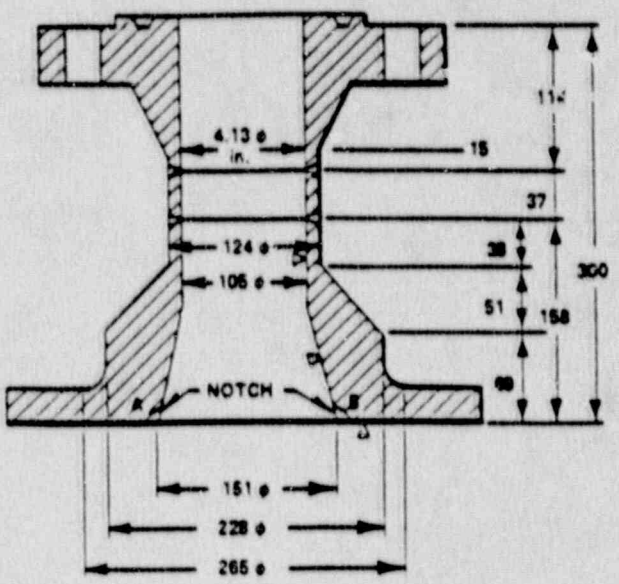

(b) CROSS SECTION OF NOZZLE TYPE N2

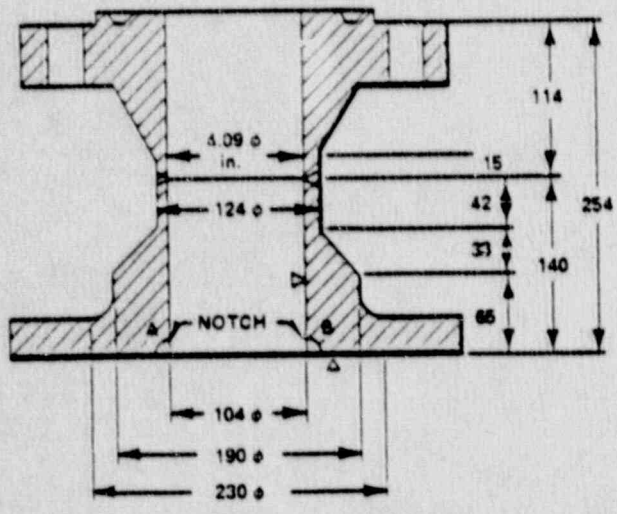

(c) CROSS SECTION OF NOZZLE TYPE N3

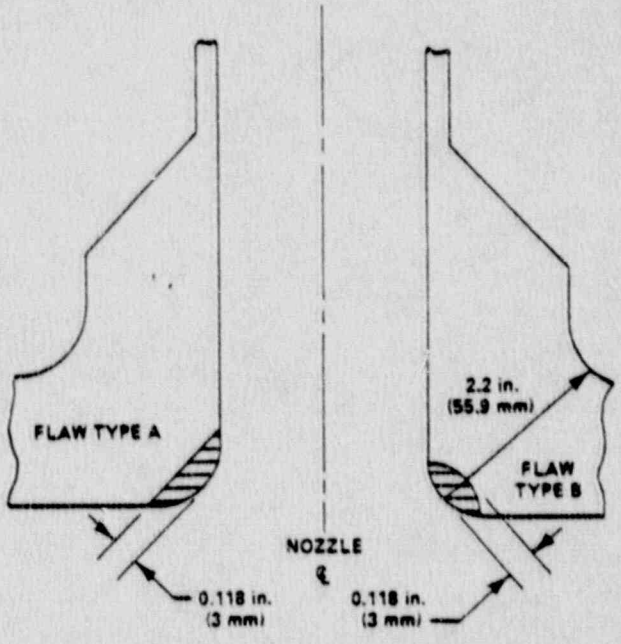

(d) MACHINED FLAW TYPE ILLUSTRATED

Fig.1 Experimental nozzle model cross sections and flaw geometries (Units in mm unless indicated otherwise)

2 The stress distribution and stress concentration factors at the blend radius for the three nozzle types were not significantly different and are in agreement with analytical data in the literature (Reference 3)

3 The crack propagation rate of the pressure vessel nozzle is dependent on the stress concentration factor of nozzle blend radius.

4 The crack propagation rate of the pressure vessel nozzle is influenced by geometry of notches (flaw type) at the nozzle blend radius.

5 General trends of crack growth obtained from the cyclic pressure test are consistent with expectations. (Crack growth rate accelerates as crack depth increases.)

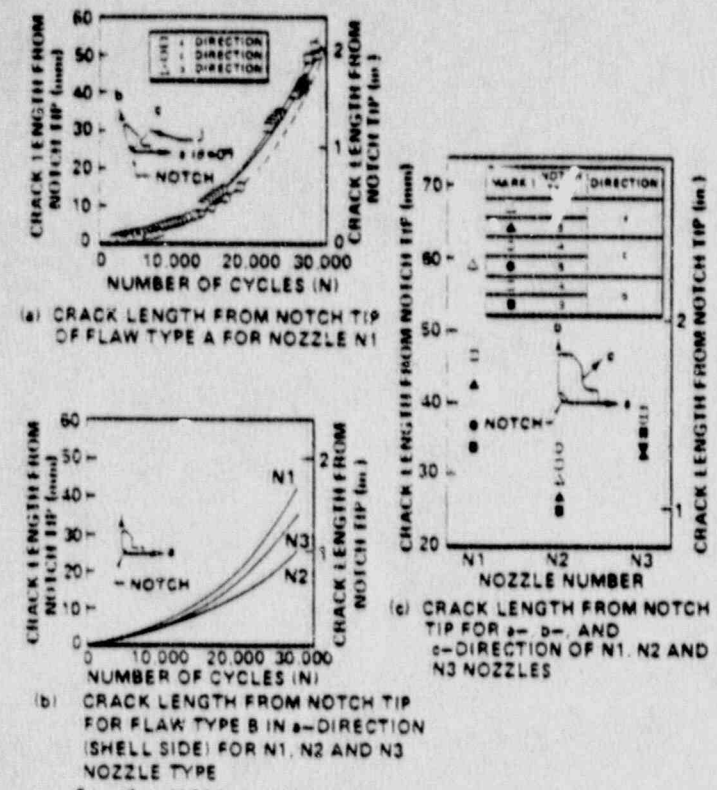

(a) CRACK LENGTH FROM NOTCH TIP OF FLAW TYPE A FOR NOZZLE N1

(b) CRACK LENGTH FROM NOTCH TIP FOR FLAW TYPE B IN a-DIRECTION (SHELL SIDE) FOR N1, N2 AND N3 NOZZLE TYPE

(c) CRACK LENGTH FROM NOTCH TIP FOR a-, b-, AND c-DIRECTION OF N1, N2 AND N3 NOZZLES

Fig.2 JAERI experimental crack growth results

FRACTURE MECHANICS EVALUATION

In order to further assess the experiment, the JAERI test results were compared with an analytical approach previously used at General Electric to evaluate BWR feedwater nozzles (Reference 4). This analytical method consists of two basic calculations. First, the stress intensity factor is determined using a polynomial curvefit approach. Secondly, the fatigue crack growth is calculated using an integration procedure. These calculations and results are described in the following sections.

Stress Intensity Factors

A general purpose, polynomial curvefit technique was used to generate stress intensity factors for the stress distributions in the nozzle (Reference 5). In this method, stress intensity magnification factors are generated for a given geometry for constant, linear, quadratic and cubic stress distributions as illustrated in Fig. 3. The stress intensity factor for any arbitrary stress distribution can then be determined by curvefitting it to a third order polynomial of the form:

$$\sigma = A_0 + A_1 x + A_2 x^2 + A_3 x^3, \qquad (1)$$

and superimposing the stress intensity factors from each term of the polynomial.

Magnification factors for several common two-dimensional geometries are available in the literature (References 5 and 6). For the feedwater nozzle, however, a set of three-dimensional magnification factors were obtained from the boundary integral equation/influence function derivation of Reference 7. As illustrated in Fig. 4, the BIE/IF nozzle corner crack simulation is simply the average of BIE/IF magnification factors developed for circular surface crack geometries in half and quarter spaces. This expression (labeled FUN 11 in Fig. 4) is used to calculate stress intensity factors in the experimental model for nozzle flaw type B (circular flaw in Fig. 1).

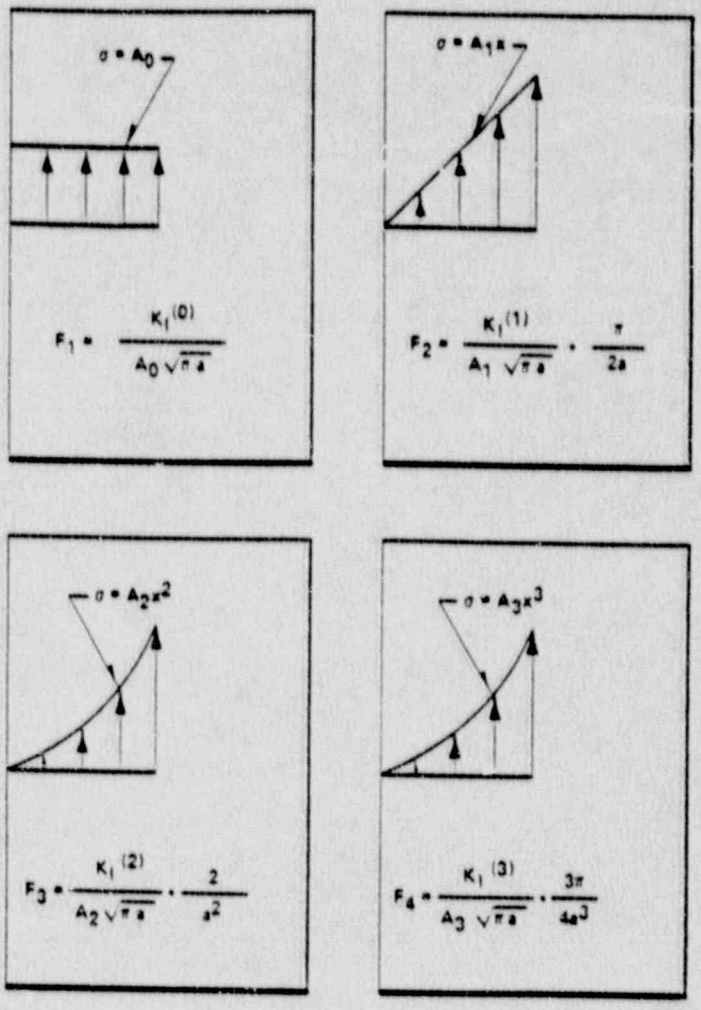

$$K_I = K_I^{(0)} + K_I^{(1)} + K_I^{(2)} + K_I^{(3)}$$

Fig.3 Stress intensity magnification factor determination

A similar expression can be used to obtain upper bound stress intensity factor estimates for the longer experimental flaw type A (straight flaw in Fig. 1). In this case, the nozzle flaw is modeled by an infinitely long crack emanating from a hole in an infinite plate (Reference 8). The solution is identical to that for a circular crack except the FUN 11 magnification factors are replaced by the FUN 8 magnification factors of Fig. 5.

Fatigue Crack Growth Evaluation

Crack Growth Data. Figure 6 presents a compilation of the fatigue crack growth data for low alloy ASTM A533B-1 steel in ambient room temperature air (Reference 9). The ASME Section XI upper-bound air crack growth curve (Reference 10) is also shown as a solid line and a best-fit crack growth curve is indicated as a dashed line on the Figure. The low alloy steels used to fabricate the model pressure vessel are very similar to A533B-1 and both air and oil are nonaggressive media. Thus, the

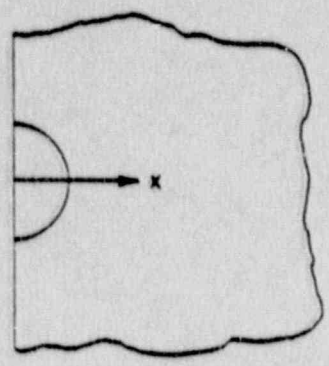

FUN 9 – SEMI-CIRCULAR CRACK IN HALF-SPACE

$$K_I = \sqrt{\pi a}\left[0.688\,A_0 + 0.522\left(\frac{2a}{\pi}\right)A_1 + 0.434\left(\frac{4^2}{2}\right)A_2 + 0.377\left(\frac{4a^3}{3\pi}\right)A_3\right]$$

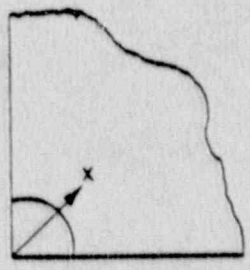

FUN 10 – QUARTER-CIRCULAR CRACK IN QUARTER-SPACE

$$K_I = \sqrt{\pi a}\left[0.723\,A_0 + 0.551\left(\frac{2a}{\pi}\right)A_1 + 0.462\left(\frac{4^2}{2}\right)A_2 + 0.408\left(\frac{4a^3}{3\pi}\right)A_3\right]$$

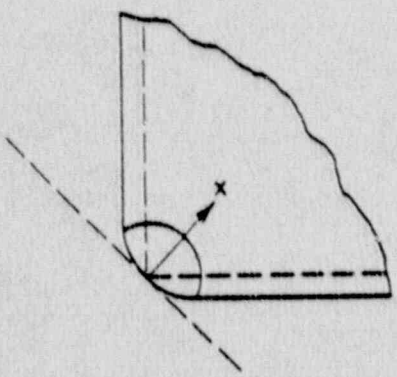

FUN 11 – SIMULATED 3-D NOZZLE CORNER CRACK

$$K_I = \sqrt{\pi a}\left[0.706\,A_0 + 0.537\left(\frac{2a}{\pi}\right)A_1 + 0.448\left(\frac{4^2}{2}\right)A_2 + 0.393\left(\frac{4a^3}{3\pi}\right)A_3\right]$$

Fig.4 Boundary integral equation/influence function magnification factors for circular nozzle flaws

curves of Figure 6 are considered applicable to the JAERI experiment.

Integration Procedure. The air environment crack growth law of Figure 6 was integrated numerically starting from the initial crack size of 3 mm (0.118 inches) to generate a crack depth versus number of cycles curve. The integration procedure was as follows:

1. Select a_0 (initial crack size)

2. $K_{max} = K_{pressure}$

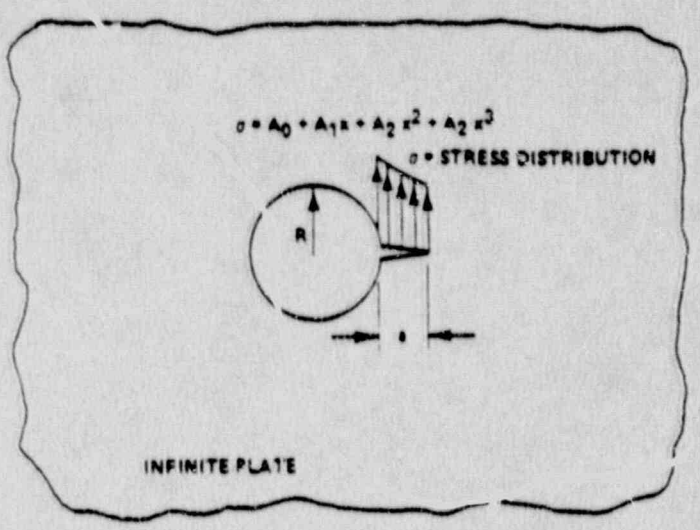

$$K_I = \sqrt{\pi a}\left[F_1\,A_0 + F_2\left(\frac{2a}{\pi}\right)A_1 + F_3\left(\frac{4^2}{2}\right)A_2 + F_4\left(\frac{4a^3}{3\pi}\right)A_3\right]$$

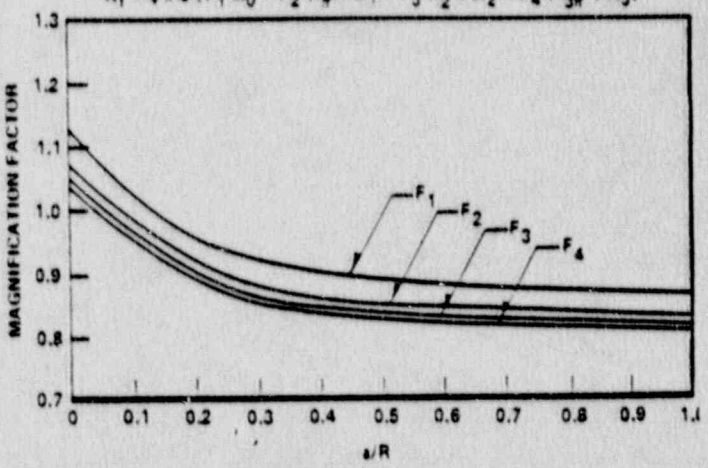

Fig.5 FUN 8 stress intensity factor solution-crack emanating from hole in an infinite plate

3. $K_{min} = 0$

4. $\Delta K = K_{max} - K_{min}$

5. $\frac{da}{dN} = (0.0267 \times 10^{-9})\,\Delta K^{3.726}$
(Sec XI upper bound air crack growth curve)

6. $\Delta a = (da/dN) \times 1$

7. $a = a_0 + \Delta a_1$

Steps 1 to 7 were repeated for each cycle, constantly incrementing the crack depth by Δa. An automatic version of the procedure was used to generate crack depth versus number of pressurization cycles. For the best-fit crack growth law case, the curve

$$\frac{da}{dN} = 0.02103 \times 10^{-9}\,\Delta K^{3.726}$$

was used in place of the crack growth law of Step 5.

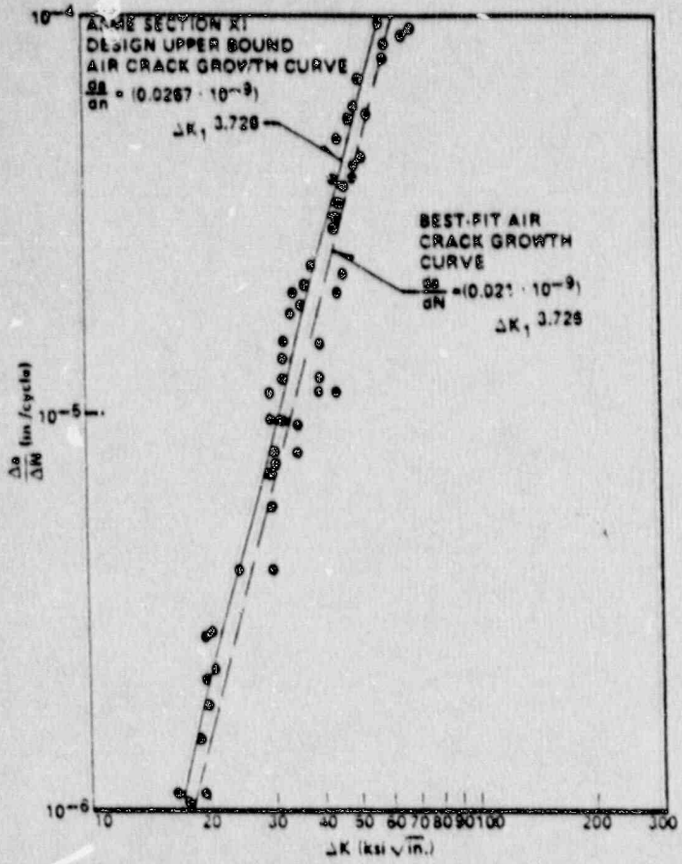

Fig.6 Wide range of fatigue crack propagation of ASTM A533 B-1 steel (Reference 9) (R = 0.10, ambient room air)(in.) = (25.4 mm);(ksi$\sqrt{in.}$) = (1.098 MN/m$^{3/2}$)

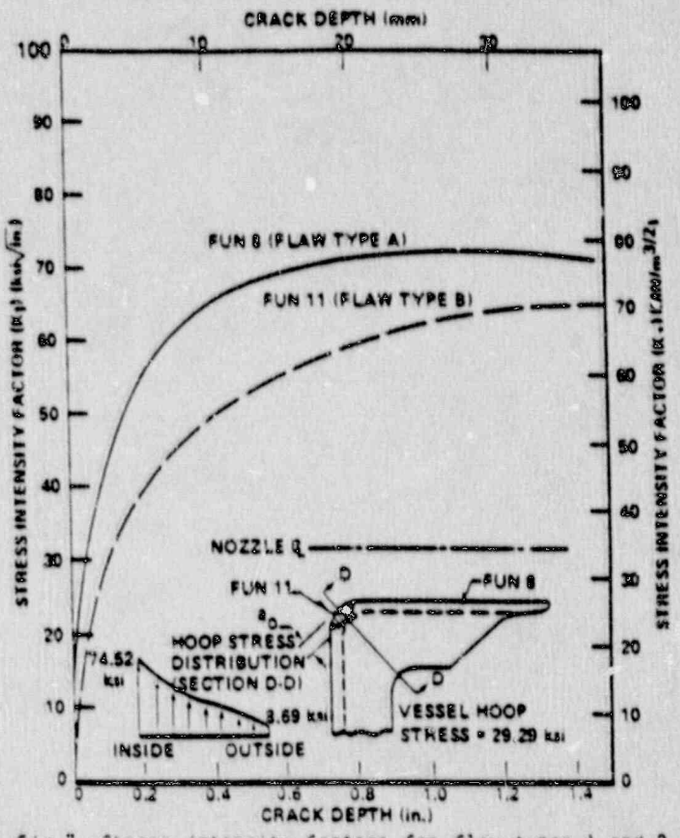

Fig.7 Stress intensity factors for flaw types A and B

Results

The fracture mechanics analytical results are graphically illustrated in Figs. 7 through 10. Fig. 7 provides a plot of stress intensity factor K_I versus crack depth for nozzle flaw type B (circular). The plot is based on the polynomial curve fit approach using FUN 11 magnification factors for a simulated nozzle corner crack as described above. A second curve is also provided based on FUN 8 magnification factors for an infinitely long crack emanating from a hole in a plate, which should provide an upper bound estimate of the experimental nozzle flaw type A (straight).

Crack growth curves based on the above stress intensity factors are provided in Figs. 8 and 9. Fig. 8 presents crack growth predictions for the circular flaw geometry (FUN 11) for both upper bound and best estimate crack growth curves. Experimental data for flaw type B in nozzles N1 and N3 are also shown for comparison. The analytical results are in excellent agreement with experiment, with the upper bound design curve providing a conservative but reasonable prediction of the test results. The best fit crack growth curve is more accurate, but slightly underpredicts the experiment in the central portion of the curve. Fig. 9 presents crack growth predictions for the infinitely long flaw geometry (FUN 8), compared to experimental data for flaw type A in nozzles N1 and N3. In this case, both the design and best fit curves significantly overpredict crack growth behavior. The type A flaw appears to

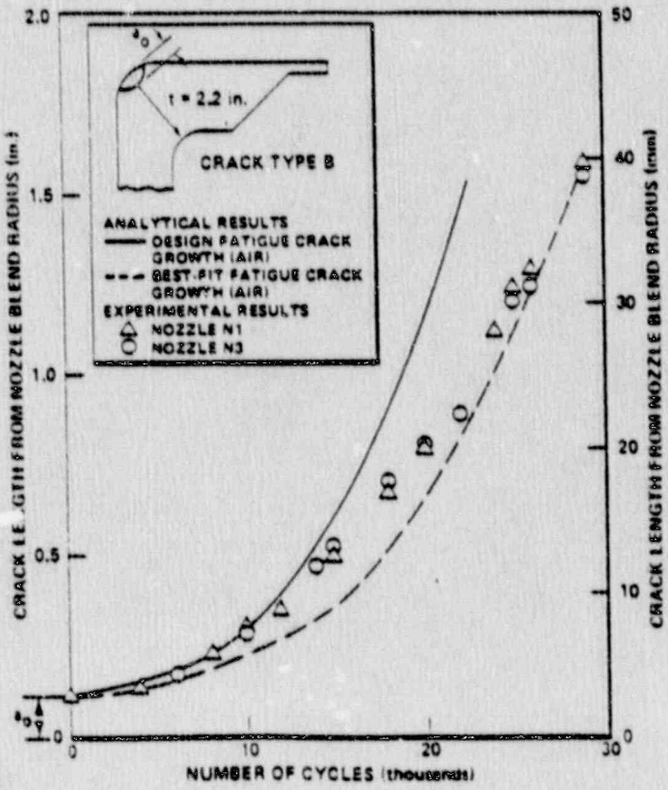

Fig.8 Flaw type B analytical and experimental crack results

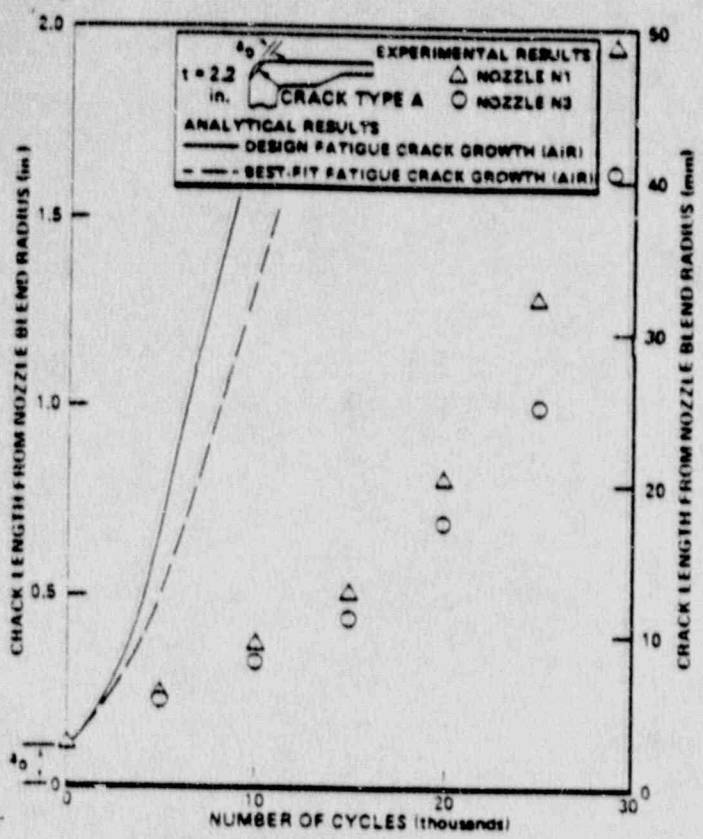

Fig.9 Flaw type A analytical and experimental results

fall between the circular and infinitely long flaw predictions, but much closer to the circular geometry as illustrated in Fig. 10, which is a comparative plot of all the data from Figs. 8 and 9.

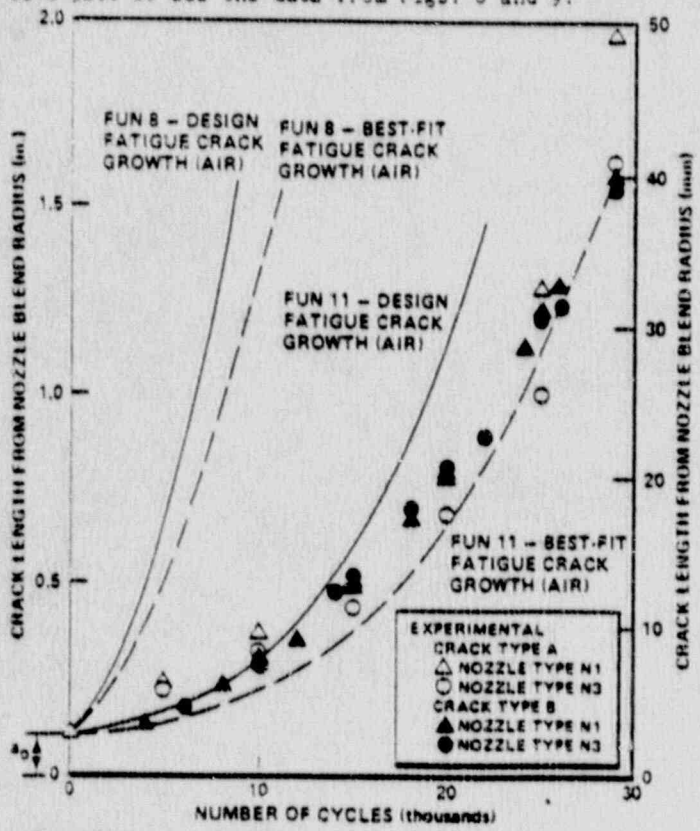

Fig.10 Summary of flaw type A and B experimental and analytical results

DISCUSSION

The air design crack growth curve analytical results of Fig. 8 were conservative but reasonable when compared to the JAERI experimental results. Since the same analytical approach has been used to predict feedwater nozzle crack growth in BWR operating plants, it is expected that a similarly good comparison will occur between BWR operating plants and analytical results.

In support of this conclusion, it is useful to point out the similarities between the experimental apparatus and BWR operating plants. Two of the experimental nozzles (N1 and N3) are similar in construction and configuration to BWR feedwater nozzles. The ASME Boiler and Pressure Vessel Code (Reference 2) was used to construct and design the JAERI experimental vessel model as well as BWR pressure vessels. The low alloy steels used in the experimental vessel are virtually the same as the material used in the construction of BWR pressure vessels. Field observations of BWR feedwater nozzle cracking have shown that most cracks which have developed are similar to flaw type B (circular) with some tending toward flaw type A (straight). In summary, the experimental apparatus and BWR pressure vessels are similar in construction, nozzle configuration, material properties and flaw geometry.

Dissimilarities between the JAERI experiment and BWR operating conditions are basically two: environment and types of cyclic loading. The experimental environment was an oil medium at ambient temperature 297K (75°F) while the BWR operating plant environment is a high purity water medium at 561K (550°F). However, this difference in environment between test and reactor can be addressed in the analysis by use of a fatigue crack growth law which is applicable in the BWR environment, for which extensive experimental data are available and are continuing to be obtained. In the JAERI experiment, the model nozzles were subjected to pressure cyclic loading only, while in operating BWRs the feedwater nozzles experience both pressure and thermal cyclic loading. However the polynomial curvefit approach is equally valid for pressure and thermal stress distributions. Assuming that the thermal cycling can be accurately defined in terms of stresses and number of cycles, its presence should not alter the accuracy of the crack growth predictions. Thus, the differences between test and reactor noted above do not invalidate the demonstrated applicability of the analytical approach. To the extent that environmental fatigue crack growth behavior and description of reactor vessel thermal cycles are known, the fracture mechanics methodology used in Reference 4 should provide accurate predictions of BWR feedwater nozzle crack growth versus reactor operating cycles.

CONCLUSIONS

In view of the excellent agreement between analytical crack growth predictions and experimental nozzle crack growth data from the JAERI pressure vessel test, and considering the similarities and differences between the test and BWR operating service, the following conclusions are drawn:

1. The test confirms GE predictions that in the unlikely event that reactor vessel nozzle cracks become very large, the vessel

failure mode which would develop is one of leak-before-break.

2 The fracture mechanics methodology used by GE to predict nozzle crack growth versus vessel operating cycles is fundamentally sound and, to the extent that environmental fatigue crack growth behavior and description of vessel thermal cycles are known, should provide accurate crack growth predictions for the entire range of crack growth, from nucleation to through-wall leakage.

These conclusions are particularly significant with regard to very large cracks (greater than 20 percent of nozzle wall thickness) for which there has been no reactor experience, and for which the applicability of the method can not be demonstrated theoretically.

REFERENCES

1 S. Miyazono, S. Uedo, T. Kodaira, K. Shibata, T. Isozaki and N. Nakajima, "Fatigue Behavior of Nozzles of Light Water Reactor Pressure Vessel Model," Third International Conference on Pressure Vessel Technology, ASME.

2 "Rules for Construction of Nuclear Vessels," ASME Boiler and Pressure Vessel Code, Sec. III.

3 J. D. Dillman and Y. R. Rashid, "Three-Dimensional Analysis of Reactor Pressure Vessel Nozzles," 1st International Conf. SMIRT Vol. 4, Part G, Sept. 1971.

4 A. B. Fife, I. R. Kobsa, P. C. Riccardella, H. T. Watanabe, "Boiling Water Reactor Feedwater Nozzle/Sparger Interim Program Report," NEDO-21480, July 1977, BWRPD, General Electric Company.

5 C. B. Buchalet, W. H. Bamford, Stress Intensity Factor Solutions for Continuous Surface Flaws in Reactor Pressure Vessels, ASTM-STP-590, 1975.

6 R. Labbens, A. Pellissier-Tanon, J. Heliot, Practical Method for Calculating Stress Intensity Factors through Weight Functions, ASTM-STP-590, 1975.

7 Private Communication, P. M. Besuner to P. C. Riccardella, Three-Dimensional Stress Intensity Factor Magnification Constants for Radial Feedwater Nozzle Cracks, Failure Analysis Associates, June 29, 1976.

8 A. S. Kobayashi, N. Polvanich, A. F. Emery, W. J. Love, "Corner Crack at the Base of a Rotating Disk," ASME Paper No. 75-WA/CT-18, April 4, 1976.

9 P. C. Paris, R. S. Bucci, E. T. Wessel, W. G. Clark, and T. R. Mager, "Extensive Study of Low Fatigue Crack Growth Rate in A533 and A508 Steels," Stress Analysis and Growth of Cracks, Proceedings of the 1971 National Symposium on Fracture Mechanics, Part I, ASTM STP 513, American Society for Testing and Materials, 1972.

10 "Rules for Inservice Inspection of Nuclear Power Plant Components," ASME Boiler and Pressure Vessel Code, Section XI.